

EXPERIMENTAL INVESTIGATION OF AN IRB 120 ROBOT THERMAL BEHAVIOR FOR HEAT SOURCES AND THERMAL FIELD DISTRIBUTION IDENTIFICATION

Constantin DUMITRAȘCU¹, Adrian Florin NICOLESCU^{2*}, Cozmin CRISTOIU³

¹⁾ PhD, Eng., Department Quality Engineering and Industrial Technologies, University "Politehnica" of Bucharest, Romania

²⁾ PhD, Prof., Department of Robots and Manufacturing Systems, University "Politehnica" of Bucharest, Romania

³⁾ Assistant professor, PhD Student, Department of Robots and Manufacturing Systems, University "Politehnica" of Bucharest, Romania

Abstract: The paper presents an original approach on experimental research on industrial robot thermal behavior. The experiments were developed in the ABB National Centre for direct and assisted programming of industrial robots, from Department of Robots and Manufacturing Systems, Faculty of Industrial Engineering and Robotics, Politehnica University of Bucharest. The experimental research had as main purpose to verify the preliminary assumptions regarding main heat sources in IR's thermal behavior and thermal field distribution on IR's main partially assemblies. The experimentally research has been conducted following up specific requirements of ISO 9283-1998 Manipulating industrial robots – Performance criteria and related test methods were focused on preliminary experimentally evaluation of an ABB IRB 140 industrial robot by mean of an infrared ThermaCam SC 640 equipment for two different speed ranges working cycles. Main results obtained from experimental research and data processing confirm initially assumption on heat sources identification and supply important information about thermal field distribution. Specific external maximum temperature of each IR's partially assembly and the thermal field distribution on each IR's partially assembly were clearly identified as well as their temperature variations along both specific programmed experimentally work cycles. Further applicative research (FEM) and experimentally works (with laser tracker system) will be performed for future evaluation of the specific thermal displacements of IR's tool center point along same working cycles.

Key words: industrial robot behavior, heat sources, thermal field distribution, infrared camera, thermal image, thermal data processing.

1. INTRODUCTION

The paper presents experimental research works performed in the "ABB National Centre for direct and assisted programming of industrial robots", Department of Robots and Manufacturing Systems, Faculty of Industrial Engineering and Robotics, Politehnica University of Bucharest on industrial robots (IR) thermal behavior.

The experimentally research has been conducted following up specific requirements of ISO 9283-1998 Manipulating industrial robots – Performance criteria and related test methods were focused on preliminary experimentally evaluation of an ABB IRB 140 industrial robot by mean of an infrared ThermaCam SC 640 equipment for two different speed ranges working cycles. The experimental research had as main purpose to verify the preliminary assumptions regarding main heat sources in IR's thermal behavior and thermal field distribution on IR's main partially assemblies.

Concerning IR's thermal behavior, external maximum temperature of each IR's partially assembly and thermal field distribution on each IR's partially

assembly as well as their temperature variations along both specific programmed experimentally work cycles have been investigated.

2. THE ABB IRB 120 ROBOT FUNCTIONAL CHARACTERISTICS AND CONSTRUCTIVE FEATURES

2.1. ABB IRB 120 functional characteristics

The experimentally tested IR – ABB IRB 120, illustrated in fig 1, has main functional characteristics presented in Table 1.

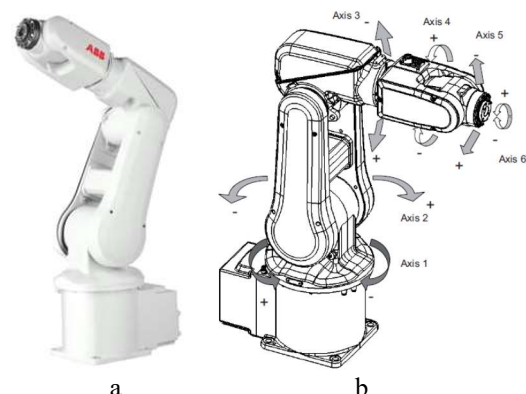


Fig. 1. ABB IRB 120 robot: a – general view; b – numerically controlled axis [1, 2].

* Corresponding author: 313 Splaiul Independentei, District 6, 06042, Bucharest, Romania,
Tel.: +40744.923.533;
Fax: +4021.269.1332
E-mail addresses: afnicolescu@yahoo.com (A. F. Nicolescu)

Table 1
ABB IRB 120 main functional characteristics [1]

Axis movement	Working range	Maximum Velocity
Axis 1	+165° to -165°	250°/s
Axis 2	+110° to -110°	250°/s
Axis 3	+70° to -110°	250°/s
Axis 4	+160° to -160°	320°/s
Axis 5	+120° to -120°	320°/s
Axis 6	+400° to -400°	400°/s
Maximum reach	Handling capacity	Repeatability
0.58 m	3 kg	0.01 mm

2.2. ABB IRB 120 specific design features

In order to having a perspective preliminary approach on IR's thermal behavior, first the specific design features of studied ABB IRB 120 were analyzed.

From this point of view the most important details on IR's internal structure as well as specific design issues related to considered robot's structural elements are presented in Figs. 2–5 [3].

For the internal structure of axis 1 and axis 2 (Fig. 1) it may be identified: 1 and 2 – fixed elements from IR base, 3 – driving motor and associated cycloid gearbox for axis 2, 4 – mobile (rotating) element of joint 1, the bottom plastic closing shield, 6 – structural element for axis 2 location against axis 1 mobile element and 7 the driving motor and associated cycloid gearbox for axis 2.

As concerns the internal structure of axis 3 (Fig. 3), supplementary to the elements already illustrated and identified in Fig. 2, from Fig. 3 it may be noticed: 1 – structural element for the first link of the articulated arm, 2 – driving motor for axis 3 equipped with the driving pulley 4 for the timing belt transmission, 3 – structural frame for motor 2 mounting, 5 – driven pulley connected to the shaft and flange connected to the second link 6 of the IR articulated arm, and the covers 7 and 8 mounted on the first link structural element.

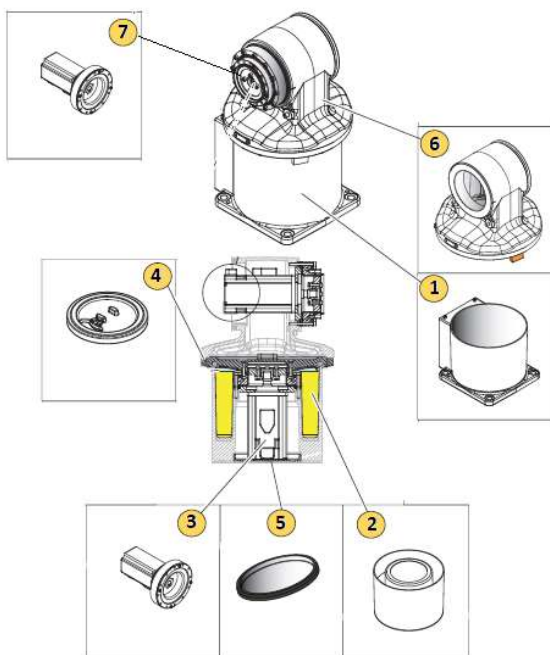


Fig. 2. ABB IRB 120 robot axis 1 and 2 internal structure and structural elements [3].

Finally, Figs. 4 and 5 present the internal structure of axis 4, axis 5 and axis 6, in two modalities: as having the driving motors (2, 4 and 5) assembled and respectively detached on / from the appropriate structural elements of IR's driven joint 4 (element 10), joint 5 (element 11) and joint 6 (element 12). The motor 2 and the associated cycloid gearbox are located in the front side of the second link of the articulated arm 1, the motor 4 and the associated timing belt transmission in the structural element 10 and the motor 5 (connected through a gearbox to the driven element 12) is located in the pitch structural element 11 (having attached the gearbox for axis 5).

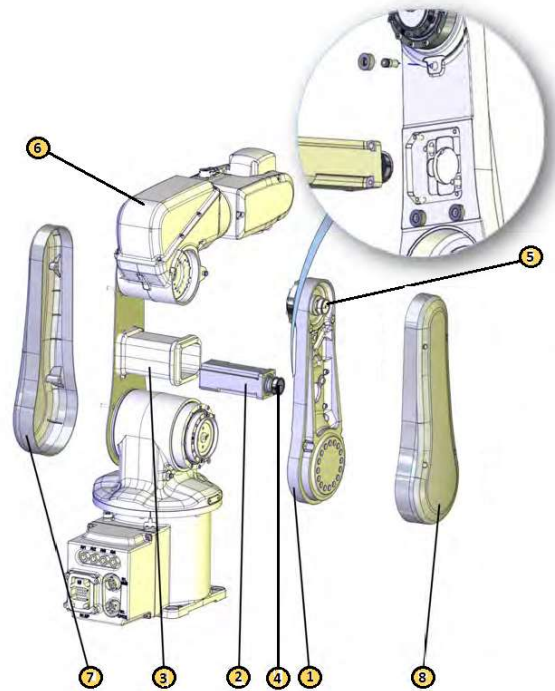


Fig. 3. ABB IRB 120 robot axis 2 and 3 internal structure and structural elements [3].

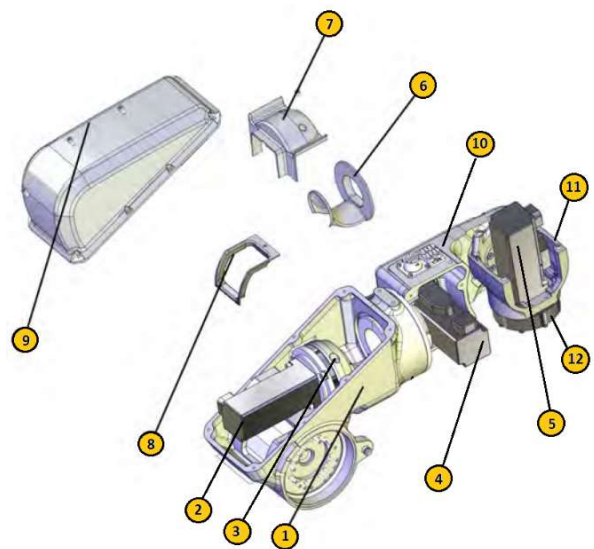


Fig. 4. ABB IRB 120 robot axis 4, 5 and 6 internal structure and structural elements (motors assembled) [3].

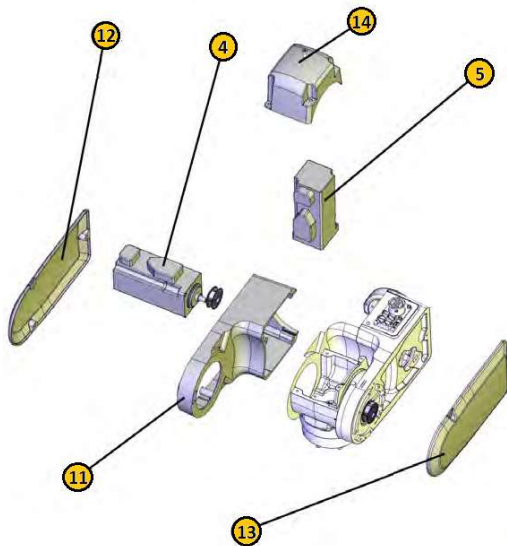


Fig. 5. ABB IRB 120 robot axis 4, 5 and 6 internal structure and structural elements (motors detached) [3].

2.3. Preliminary assumptions regarding main heat sources and issues influencing the robot thermal behavior

Concerning previously presented elements from IR's internal structure and its specific design some technical considerations are necessary to be made:

- all structural elements supporting the gravitational and inertial loads along IR's functioning are made from casted aluminum alloy (as is the case for elements 1, 2, 4 and 6 from Fig. 2, elements 1 and 3 from Fig. 3, and elements 1, 10 and 11 from Figs. 4 and 5);
- some elements, generally covers and auxiliary support frames of the IR are made from plastic materials (as in the case for elements 5 from Fig. 2, elements 7 and 8 from Fig. 3, elements 6, 7, 8 and 9 from Fig. 4, and elements 12–14 from Fig. 5);
- the cycloid gear boxes associated to the driving motor from axis 1, axis 2 and axis 4 are made for high alloyed steel, (besides for axis 3 and axis 5 they are replaced by timing belt transmission and respectively a direct drive solution for axis 6).

Considering previously specified technical aspects some estimative assumptions related to the further IR's thermal behavior analysis may be also formulated:

- the purpose of the experimental research is to identify the most important heat sources and respectively the thermal field distribution along IR's partially assemblies including too the identifying of the external temperature main IR's components;
- as generally known from technical literature review [4–8], and previously own researches [9], a preliminary assumption regarding the most important heat sources in IR' thermal behavior are expected to be identified on axis 1–axis 6 IR's driving motors level. Complementary (however, less important) heat sources are expected to be identified also on cycloid gearboxes level included in axis 1, axis 2 and axis 4.
- as concerns the heat transfer along IR's overall structure the principal means for the heat transfer may be considered conduction and radiation. Heat transfer by convection may be excluded from IR's thermal behavior evaluation because, (in the absence of an air

recirculation system for internal IR's forced cooling) it has a very limited effect;

- it is also expected as the thermal conduction effect will miss from IR components made from plastic materials (due to their reduced thermal conductivity) the possible evidence of some heating of such IR elements being due exclusively to IR internal heated parts radiation effects.

3. THE EXPERIMENTAL SETUP

3.1. The experimental equipment

In order to evaluate ABB IRB 120 robot thermal behavior an infrared ThermoCam SC640 camera (figure 6) has been used [10].

The infrared ThermoCam SC640 is a thermal detector system used in applications for thermal evaluation in the field of microelectronics, telecommunications, paper processing, automotive, plastics manufacture, injection molding, mechanical testing and others. The Camera can register thermal models in real time. The sensor which the camera is equipped has a resolution of 640x480 pixels. The images acquired by the camera can be processed with the software, "ThermoCam Researcher" (for PC). Static or kinematic images can be analyzed frame to frame or in real time. Image processing is done using integrated measuring functions: spot temperature, temperature linear profiles, temperature histograms per areas or lines, identification of minimum or maximum temperature from a specific point, line or area etc.

The experimental setup with the ABB IRB 120 tested robot and the ThermoCam SC640 is presented in Fig. 5 and technical characteristics of the ThermoCam SC640 are synthetically resumed in Table 2 [10].



Fig. 6 The IR ThermoCam SC640 [10].



Fig. 5. Experimental setup for ABB IRB 120 robot thermal behavior analysis.

Table 2

Technical characteristics of the ThermaCam SC640 [10]

Thermal imaging performance	
Thermal sensitivity	30 mK la 30°C
Zoom	8x
Thermal accuracy	±2°C
Temperature measuring range	-40°C la +2000°C
Spectral range (wavelength)	7.5 la 13µm
Maximum number of simultaneously measuring points	10
Maximum number of measuring areas	5
Linear measuring profile	Free line orientation
IR Resolution	640x480 pixels
Operation image frequency	120Hz
Measuring image analysis	
Isothermal	Identification of all points having temperatures between two preset limits
Temperature differences	The difference of the temperatures between two distinctive point of the image
Warm / cool automated detection	Automated indication of points having the maximum and minimum temperature from a selected surface
Reference temperature	Manually set or automated camera acquired
Emissivity correction	Manually selection for different types of material surfaces
Measurement correction	Manually correction for reflected temperatures and atmospheric IR transmission
Environment specifications	
Operating environment temperature	-15° la +50°C
Humidity limits for operation	IEC 68-2-30/24 h 95% relative humidity
Communication interfaces	
1394 Firewire	Real time 14 bytes radiometric transmission
USB-A	For memory stick USB devices
USB-mini-B	For PC connections
Video composite	PAL / NTSC
IrDA	For data / text transmission from a PDA

3.2. The experimental procedure description

The experimentally research of the ABB IRB 140 industrial robot has been conducted following up specific requirements of ISO 9283-1998 Manipulating industrial robots – Performance criteria and related test methods were focused on preliminary experimentally evaluation by mean of an infrared ThermaCam SC 640 equipment for two different speed ranges working cycles. For performing the experimental tests, a payload of 0.3 kg for the robot was used (10% from the maximum payload of 3 kg). For the first stage of experiments the first IR's working cycle has been set by operating the robot on a maximum velocity of 0.8 m/s (50% from maximum available speed) and for the second stage of experiments the second IR's working cycle has been set to operate the robot at 1.6 m/s (100% of maximum available speed). Both working cycles were set to continuously activate in

motion all six axes of the IR up to about 75% of the maximum stroke's limits (due to the limited IR's enclosure dimensions). Each of the two stages of experiments have been performed along 3 hours of IR's continuously functioning at the same speed and by continuously registration of its thermal behavior by ThermaCam SC640. For any individual experiment stages the total IR's thermal behavior registration includes 14 sequences of 3000 images each, with an acquisition rate of 3.75 images / sec, any experiment stage including a total number of 42.000 thermograms).

Along the experimental research the atmospheric temperature from the ABB laboratory environment was 19°C, and the humidity was 40%.

For performing the experiments, the emissivity coefficient of IR ThermaCAM SC 640 was experimentally set to $\epsilon = 0.88$, the color pallet was set as RAIN and the main temperature measuring interval was set for 0°C and 500°C. Inside this measurement temperature range, for successive data processing the temperature interval from 25°C to 55°C was set for both experimental stages, in order to allow identical conditions for data processing and the thermal interpreting result's compatibility between the two working cycles.

4. THE EXPERIMENTAL RESULTS**4.1. First stage of experiments (performed with 50% of maximum available speed)**

As previously mentioned for the first stage of experiments the first IR's working cycle has been performed with a payload of 0.3 kg for the robot (10% from the maximum payload of 3 kg) and was set to continuously activate in motion all six axes of the IR up to about 75% of the maximum stroke's limits and to operate the robot on programmed trajectory with a maximum velocity of 0.8 m/s (50% from maximum available speed).

The total time of the experiment has been of 3 hours of IR's continuously functioning at the same speed and by continuously registration of its thermal behavior by ThermaCam SC640, based on previously preliminary experiments looking for identifying the thermal stability time – level reach (temperature stabilization interval for IR heat distribution).

The representative set of thermal images acquired along first working cycle performed on the end of the total first experimental stage time (of 3 hours) is presented in Fig. 6. Thus, from Fig. 6, according to the specific design features and internal structure of the ABB IRB 120 robot (previously presented in section 2) the full set of thermal images allow to highlight the confirmation of the first preliminary assumption regarding the identifying of IR's driving motors as being the most important heat sources in robot thermal behavior (the highest registered temperatures being identified around driving motors specific location).

A second confirmation of the preliminary assumptions is related to the heat transfer phenomena along IR's overall structure. As preliminary estimated the

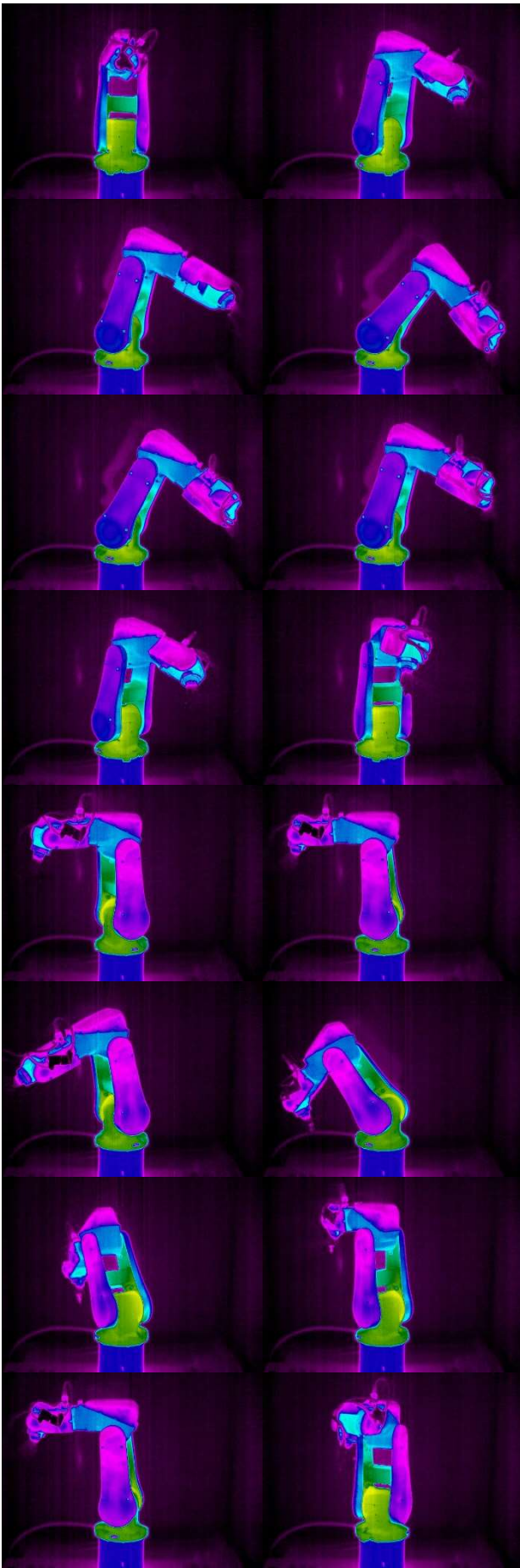


Fig. 6. Experimental working cycle for stage 1 of experiments in ABB IRB 120 robot thermal behavior analysis.

principal means for heat transfer are the conduction and radiation phenomena (the structural components made from aluminum alloy being the most influenced elements and the plastic material components of the IR being the less influenced elements by thermal field distribution).

As it also may be observed from Fig. 6, that greater temperature ranges in IR functioning may be identified in the driving motor of axis 2 and axis 3 proximity areas (first three IR's axis driving motors supporting main inertial loads in IR's operation). However, jointly to above observations, some special remark is necessary to be made for the registered temperature in the proximity area of the driving motor for axis 1: the reduced temperature of the base rotation module's external surface (in blue) versus the temperature of the proximity area of the driving motor for axis 2 (in yellow-green) may be explained by the internal design of base rotation module, as being due to the specific design shapes of element 2 from figure 2 (representing a thermal barrier against thermal radiation phenomena for the heat generated by axis 1 driving motor through the external surface of the module). From this point of view, the real temperature of the driving motor for axis 1 is expected to be greater than or at least just near the temperature of driving motor for axis 2, (due to the increased inertial loads applied to axis 1 driving motor versus the inertial loads applied to axis 2 driving motor).

In these conditions, as it may be see from figure 6 the maximum temperature registered along first experiment is for the area where are located the axis 2 driving motor and the associated cycloid gearbox (marked in green-yellow color), followed up, (with a low decrease in temperature), by the area where is located the axis 3 driving motor. However as concerns the registered thermal field distribution (temperature gradient) for the first area, some supplementary remark is necessary to be made: the temperature of the external surface of IR's 2-nd axis rotation module mostly illustrated in green increase through yellow for one side illustrating the overheating of yellow area versus the green area. This may be explained as having two causes. First of them is related to the heat conduction process allowed by the direct contact between the structural element of the link 1 of the articulated arm (made from aluminum alloy) with the cycloid gearbox (made from alloyed steel) associated the driving motor for axis 2. The second cause is related to the supplementary heating generated by the cycloid gearbox that add a complementary increasing of the temperature of the same area (marked by yellow color).

In the same time regarding the heat distribution on the rest of IR's elements, from Fig. 6 it may be observed that the aluminum structural element of the 1st link of the articulated arm (mostly green on the inside surface located near the driving motors for axis 2 and 3) is more warmed than the aluminum structural element of 2nd link of the articulated arm (mostly marked in blue), illustrating the greater amount of heat transferred from the driving motors of axis 2 and 3 to the 1-st link than the amount of heat transferred from the driving motors of 4, 5 and 6 axis to the 2nd link. Similarly, regarding the components of the IR made from plastic materials (covers for 1st link and 2nd link) almost all components are marked in same color (indigo) excepting the lower

area of the cover 8 (joined with the structural element of link 1) which has an increased temperature (marked in blue) in the area previously highlighted as having the maximum temperature (near driving motor and gearbox of axis 2).

4.2. Second stage of experiments (performed with 100% of maximum available speed)

As also previously mentioned for the second stage of experiments the second IR's working cycle has been performed with the same payload of 0.3 kg for the robot (10% from the maximum payload of 3 kg) and was set to continuously activate in motion all six axes of the IR up to about 75% of the maximum stroke's limits and to operate the robot on programmed trajectory with a maximum velocity of 1.6 m/s (100% from maximum available speed).

The total time of the second experiment has been also of 3 hours of IR's continuously functioning at the same speed and by continuously registration of its thermal behavior by ThermaCam SC640, looking for identifying the thermal stability time – level reach (temperature stabilization interval for IR heat distribution).

The representative set of thermal images acquired along the second working cycle performed on the end of the total second experimental stage time (of 3 hours) is presented in Fig. 7. Similarly with previous experiment, from Fig. 7, accordingly with the specific design features and internal structure of the ABB IRB 120 robot (previously presented in section 2) the full set of thermal images allow to highlight once again the confirmation of the first preliminary assumption regarding the identifying of IR's driving motors as being the most important heat sources in robot thermal behavior (the highest registered temperatures being identified around driving motors specific location).

Beside of this, a second confirmation of the preliminary assumptions related to the heat transfer phenomena along IR's overall structure is once again confirmed. As preliminary estimated the principal means for heat transfer are the conduction and radiation phenomena (the structural components made from aluminum alloy being the most influenced elements and the plastic material components of the IR being the less influenced elements by thermal field distribution).

However, as was expected, between first and the second experiment it may be remarked the overall increasing of corresponding (specific) temperatures for all investigated areas of each IR's structural element. This increasing in temperature of IR's structural elements is more pregnant on external surfaces of the first three IR's modules corresponding to axis 1, axis 2 and axis 3, where the increasing of the working cycle execution speed is leading to the increasing of the resistant (inertial) torques applied to the driving motors and gearboxes and, as result of the load overcharging the overheating of these IR's elements may be remarked.

As concerns the thermal field distribution as Fig. 7 present, that greater temperature ranges in IR functioning may be identified again in the proximity areas of the driving motor of axis 2 (now in red-white) and axis 3 (in yellow-green) due to the fact that first 3 IR's axis driving motors are supporting main inertial loads in its operation.

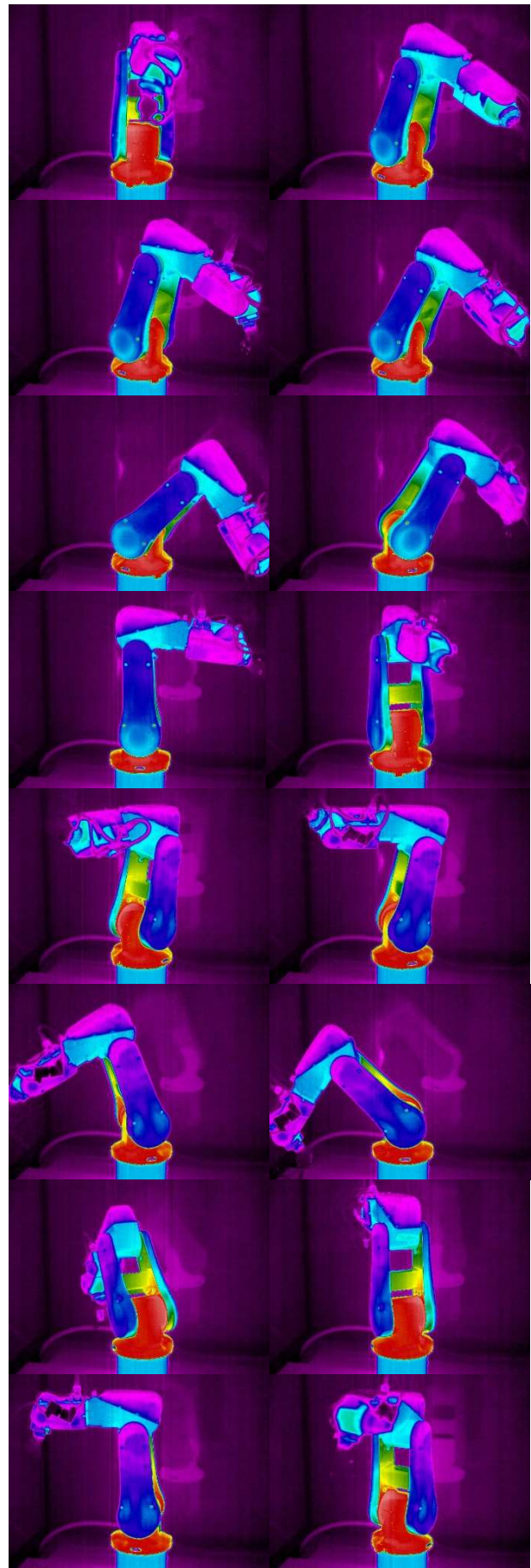


Fig. 7. Experimental working cycle for stage 1 of experiments in ABB IRB 120 robot thermal behavior analysis.

Complementary slightly increasing in temperature may be also remarked on 4th axis driving motor and gearbox level (now in blue – white comparatively with previously dark blue).

However, similarly to previously above observations, some special remark is necessary to be made for the registered temperature in the proximity area of the driving motor for axis 1: the reduced temperature of the base rotation module's external surface (now in white-blue instead of dark blue, thus more warmed than previously) versus the temperature of the proximity area of the driving motor for axis 2 (now in red – white instead of yellow-green, also more warmed than previously) may be explained by the same internal design of base rotation module, as being due to the specific design shapes of element 2 from figure 2 (which represent a thermal barrier against thermal radiation phenomena for the heat generated by axis 1 driving motor through the external surface of the module). From this point of view, the real temperatures of the driving motor for axis 1 and associated gearbox are expected to be greater than the temperature of driving motor for axis 2 and associated gearbox, (due to the radically increased inertial loads applied to axis 1 driving motor versus the inertial loads applied to axis 2 driving motor by increasing the execution speed of the working cycle from 50% to 100% of IR's maximum allowable speed).

In these conditions, as it may be saw from figure 7 the maximum temperature registered along second experiment is for the same area, where are located the axis 2 driving motor and the associated cycloid gearbox (marked in red-white color), followed up, (with a low decrease in temperature), by the area where is located the axis 3 driving motor (now in green-yellow). However, as concerns the registered thermal field distribution (temperature gradient) for the first area, same supplementary remark is necessary to be made: the temperature of the external surface of IR's 2-nd axis rotation module, (mostly illustrated in dark-red increase through red-white for one side), shows the overheating of red-white area (where is also located the gearbox and the front side of the driving motor of 2-nd axis) versus the dark-red area (where is located the rear side of the drive motor). This may be explained as having same two causes as previously highlighted. First of them, related to the heat conduction process allowed by the direct contact between the structural element of the link 1 of the articulated arm (made from aluminum alloy) with the cycloid gearbox associated the driving motor for axis 2 (made from alloyed steel), and the second one, related to the supplementary heating generated by the cycloid gearbox (now more pregnant) that is adding a complementary increasing of the temperature of the same area (presently marked by red-white color).

Supplementary to previously case of experiments from Fig. 7 it may be remarked an increased warming of the area where is located the driving motor for axis 3. This area is colored from green, to yellow and respectively yellow-red starting from the rear side of the driving motor for axis 3 and going to the front side of the driving motor which is connected to the structural element of link 1. In the same time regarding for the heat distribution on the rest of IR's elements, from Fig. 7 it

may be observed that the aluminum structural element of the 1-st link of the articulated arm is marked with dark-red color on the area located just near driving motor and gearbox for axis 2, then pass to yellow in the contact area with the driving motor of axis 3, and finally to green on the inside surface located near the 2-nd link of the articulated arm, clearly showing the heat distribution as well as major effect of heat transfer by conduction phenomena from the identified heat sources through the most warm areas of the structural element of link 1.

However, it may remark too that the aluminum structural element of link 2 (mostly marked in blue), is less warmed than the structural element of 1-st link of the articulated arm illustrating the greater amount of heat transferred from the driving motors of axis 2 and 3 to the 1-st link than the amount of heat transferred from the driving motors of 4, 5 and 6 axis to the 2-nd link. Similarly, regarding the components of the IR made from plastic materials a warming through radiation phenomena may be remarked especially for covers for 1-st link of the articulated arm (the one disposed the same side with the connection the driving motors of axis 2 and 3 with this link being white-blue in the bottom area where the maximum heat conduction phenomena from driving motor and gearbox of axis 2 is present and dark blue through its upper side near the connection joint with 2-nd link and associated gearbox for axis 3). The rest of almost all components from the 2-nd link are marked mostly in same color (indigo) excepting some areas (marked in white-blue) where they locally warmed through radiation phenomena from the driving motors and the gear boxes for axis 4, axis 5 and axis 6.

As may be observed from Fig. 7, for the second experimental stage the greater temperature ranges in IR functioning may be also identified in the driving motor of axis 2 and axis 3 proximity areas (first three IR's axis driving motors supporting main inertial loads in IR's operation). Jointly to these observation, same special consideration is necessary to be made for the registered temperature in the proximity area of the driving motor for axis 1: the reduced temperature of the base rotation module's external surface (this time in white-in blue) versus the temperature of the proximity area of the driving motor for axis 2 (in red and white-red) may be explained by the internal design of this module, (the specific design shapes of element 2 from Fig. 2 representing a thermal barrier against thermal radiation phenomena for the heat generation by axis 1 driving motor). From this point of view, the real temperature of the driving motor for axis 1 is expected to be greater than the temperature of driving motor for axis 2, (due to the increased inertial loads applied to axis 1 driving motor versus the inertial loads applied to axis 2 driving motor along this second working cycle).

4.3. Processing and interpretation of experimental results for the two stages of experiments

Following previously qualitative interpretations specific numerical results have been obtained from data processing of both experiments, allowing to quantitatively characterize IR's thermal behavior and previously mentioned heat transfer phenomena as presented in Figs. 8–10.

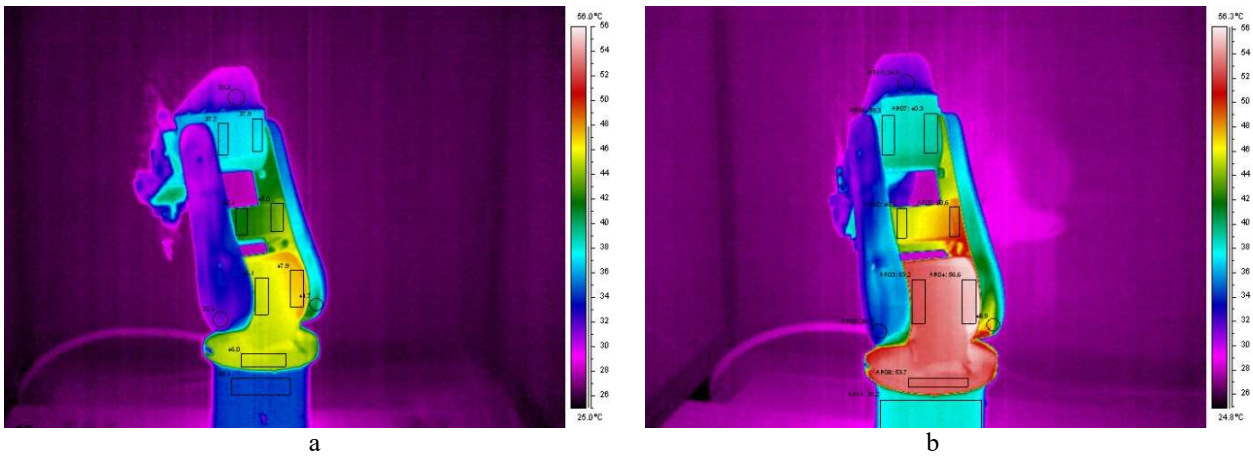


Fig. 8. Thermal field distribution on ABB IRB 120 robot along the two experimental working cycles for thermal behavior analysis and marks on major area of interest for evaluation specific temperatures of IR's partially assemblies:
a – Robot on the end of first experimental stage (working cycle performed with 50% of maximum velocity);
b – Robot on the end of second experimental stage (working cycle performed with 100% of maximum velocity).

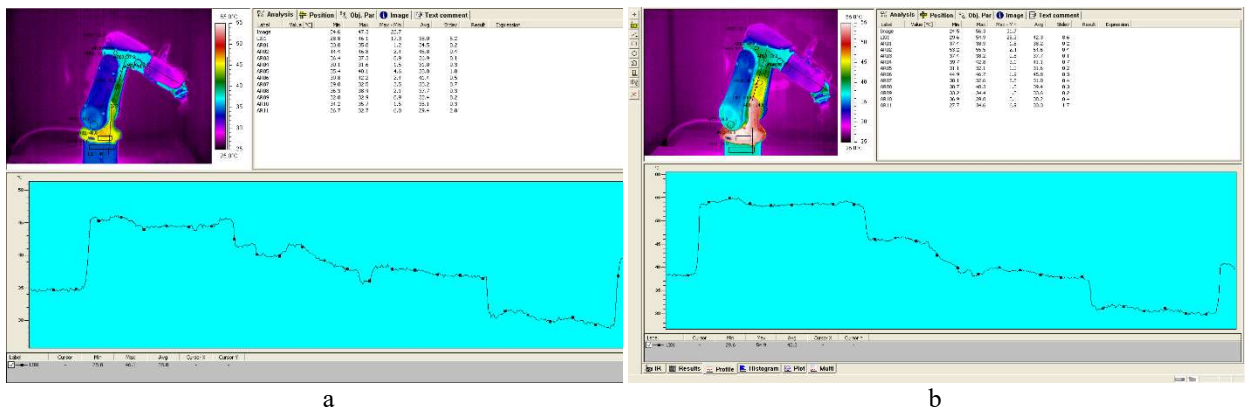


Fig. 9. Thermal field distribution on ABB IRB 120 robot along the two experimental working cycles for thermal behavior analysis and temperature variation along a single temperature line passing through all major IR's modules for evaluation of the overall temperature's variations along IR's partially assemblies:
a – Robot on the end of first experimental stage (working cycle performed with 50% of maximum velocity);
b – Robot on the end of second experimental stage (working cycle performed with 100% of maximum velocity).

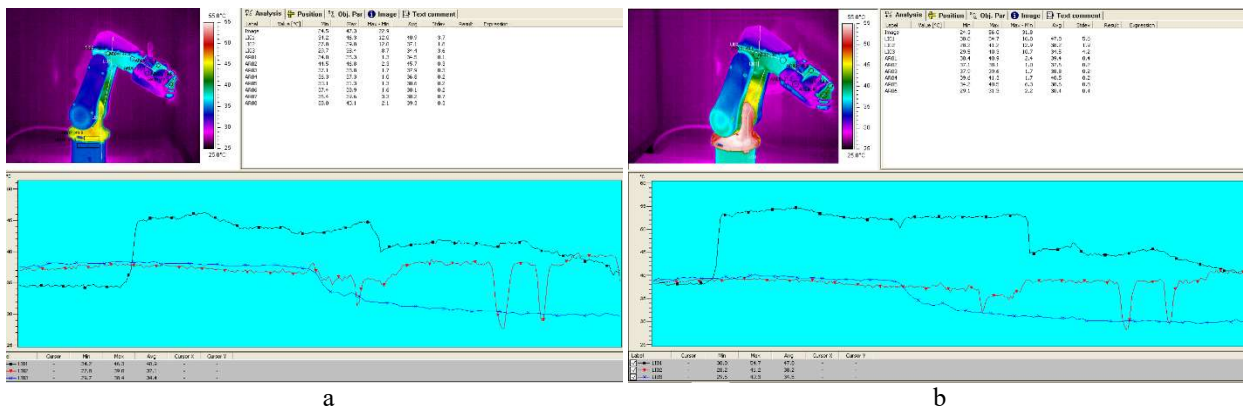


Fig. 10. Thermal field distribution on ABB IRB 120 robot along the two experimental working cycles for thermal behavior analysis and temperature variation along three temperature lines passing through all major IR's modules for evaluation differences between the specific temperatures of IR's partially assemblies:
a – Robot on the end of first experimental stage (working cycle performed with 50% of maximum velocity);
b – Robot on the end of second experimental stage (working cycle performed with 100% of maximum velocity).

In Figs. 8–10 for an easily comparison of quantitative results specific numerical data processing is presented in parallel for the two stages of experimental research performed with 50% and of maximum allowable IR speed / velocity.

First, Fig. 8 comparatively presents the thermal field distribution on ABB IRB 120 robot along the two experimental working cycles for thermal behavior analysis and marks on major area of interest for evaluation the most important specific temperatures areas of IR's partially assemblies. From this point of view, it was considered as being of maximum interest 8 area on IR's structural elements made from cast aluminum alloy (marked by rectangular shapes) and 3 areas on complementary elements made from plastic materials (marked by circular shapes).

The specific temperatures of all 11 areas of interest have been investigated by temperature lines data processing method and resultant graphical and numerical registration are presented in parallel in Fig. 9 using a single temperature line for evaluation of the overall temperature's variations along IR's partially assemblies and figure 10 using three temperature lines passing through all major IR's modules for evaluation differences between the specific temperatures of IR's partially assemblies.

As concerns now the quantitative evaluation of studied ABB IRB 120 IR thermal behavior, it may be observed that the maximum registered temperature on the external surfaces of IR (in the right side area of the driving motor and associated gear box for axis 2), along first stage of experiments (with 50% of maximum speed) was 47.9°C (Fig. 8,a) versus a 56.6°C (Fig. 8,b) maximum temperature registered along the second stage of experiments (with 100% of maximum speed), thus the increasing by 50% in execution speed of the same working cycle was followed up by an increasing of the maximum temperature of the IR by 18% (due to the increasing of the inertial loads supported by the driving motors and associated gearbox). Comparatively with the maximum registered temperature of the right sides area of driving motor and gearbox for axis 2, the corresponding lowest registered temperatures of left sides of the same areas were 45.1°C (Fig. 8,a) and respectively 53.2°C (Fig. 8,b) showing a decreasing of the temperature gradient along the external surface of IR's module including above mentioned components during the second experiment stage up only 12%, that illustrates an increased quantitative effect of heat transfer by conduction then by radiation phenomena from this partially assembly to the structural element of link 1.

Second, concerning the specific areas characterizing the thermal field distribution around the specific location of driving motor for axis 3 it may be remarked a different warming on the same right side (where the driving motor for axis 3 is connected with the structural element of link 1) versus the left side of the structural element including this motor. For the right side (much more warmed) the registered temperatures were 47.9°C in Fig. 8,a and 56.6°C in Fig. 8,b, versus the left side area (having a lower temperature) corresponding to a registered temperatures of 45.1°C in Fig. 8,a and 53.2°C in Fig. 8,b. The differences in temperatures between the left and

right sides of the structural element including the driving motor for axis 3 are in both cases of experiments the same (18%) showing an increased quantitative effect of heat transfer by conduction then by radiation phenomena from this second partially assembly through the structural element of link 1. In the same time regarding the maximum temperatures registered for this partially assembly along the two stages of experiments a difference from 47.9°C (Fig. 8,a) up 56.6°C (Fig. 8,b) may be remarked, thus by 18%, illustrating the same increasing of heat generation of driving motor for axis 3 when skip from 50% of maximum execution speed to 100% of maximum execution speed. The similarity in ration percentage for the increasing in heat generation for this driving motor of axis 3 with the driving motor of axis 2, along the two different working cycles may be interpreted as a conjugated effect of two contradictory factors. First of them is the decreasing of the inertial load for this driving motor, in comparison with the inertial load applied to the driving motor of axis 2, (that normally is expected to be reflected in a decreasing of the heat generation in the driving motor of axis 3, versus the heat generation in the driving motor for axis 2). The second one, is the drastically decreasing of the motor size for axis 3 versus the size of the motor for axis 2 that normally is expected to be reflected in an increasing of the heat generation for the driving motor for axis 3 comparatively with the driving motor of axis 2. However, beside of these two contradictory factors of influence, the presence of a gearbox in axis 3 associated with this motor allow to have a final large amplifying of the torque supplied by the motor up the necessary level for its compliance with the applied inertial load and in the same time to reduce the overheating of the driving motor of axis 3 even it drastically decrease in size / allowable torque as driving motor for axis 2.

From combination of these influence factors the result is a maximum overheating of the driving motor for axis 3 with 18% between the two experiments, showing that the motor for axis 3, even support a lower inertial load than motor for axis 2, is much more overheated due to its drastically reducing in size than the driving motor of axis 2, but however due to the associated gearbox existing in this axis the torque amplifying is still sufficient to not overpass the maximum heating – by same 18% – of the driving motor of axis 2.

Apart from these, the much lower temperatures registered on base rotation module external surfaces need to be understated as being the result of a deficient heat transfer from the driving motor and associated gearbox for axis 1, through the external surface of the base rotation module (due to previously explained influence of the thermal shield represented by the air existing in the specific shape of element 2 – presented in Fig. 2). As result the two corresponding areas located on the base rotation module of the robot, register lower temperatures of only 35.1°C (Fig. 8,a) versus a 39.2°C (Fig 8,b) illustrating an increasing in external temperature of 11.6% between the experimental stages.

As concerns the structural elements corresponding to the 1st link and 2nd link of the articulated arm of the robot, the maximum temperature of the 1st link structural element is registered along both experiments in the

proximity area of the gearbox for axis 2 location the registered temperatures being 45.1°C after the first stage experiment and respectively 48.9°C after the second stage experiment, thus an increasing of the registered temperature by 8.4% between the two experimental stages may be noted for this structural element. Next temperatures of interest, in descending range, are for the area located near the proximity of driving motor for axis 3 flange connection with the structural element of link 1 (mid of the length of link 1), where the registered temperature on the end of first experimental stage was 45°C and after the second experimental stage 50.6°C highlighting an increasing in temperature of 12.4% is remarked and respectively the area near the gearbox of axis 3 (top of the length of link 1) where the registered temperature on the end of first experimental stage was 42°C and after the second experimental stage 46°C highlighting an increasing in temperature of 9.5%.

With respect to previously highlighted percentages of temperatures increasing between the two experiment stages of 8.4%, 12.4% and 9.5% it may be noted that the increased percentage in the mid area of the 1st link structural element may be explained by the increased heat transfer by conductivity phenomena existing in this area due to the direct contact between axis 3 driving motor flange (major heat source from the area) and the structural element of link 1.

As concerns the thermal field distribution on the structural element of link 2, Fig. 8 illustrates the registered temperatures for only the rear side of this element as being between 37.7°C–37.9°C on the end of first experiment stage and 39.3°C–40.3°C on the end of the second experimental stage, showing an increasing of the temperature by only 5.3%. This reducing in the amount of heat generation and structural element warming in its rear side area is due to the reduced inertial load applied to the driving motor of axis 4, (that represent the major heat source for this structural element thermal behavior) along both experimental stages. Continuing the investigation of thermal field distribution on the 2nd link of articulated arm, further maximum registered temperatures may be highlighted as decreasing up to 35.4°C (for first experiment stage) and respectively to 38.2°C (for second experiment stage) in the front side of the 2nd link area (where is located the gearbox associated to the driving motor for axis 4 which highlights and increasing of the temperature by 8% between the two experimental stages. The registered temperatures are in the same range for the structural element 10 (presented in Fig. 4) in the area including the driving motor and associated gearbox for axis 5 which reach 37.4°C (for first experiment stage) and respectively to 37.9°C, but are significantly increasing for the structural element 11 (presented in Fig. 4) in the area including the driving motor and associated gearbox for axis 6 which reach 46.1°C (for first experiment stage) and respectively to 54.9°C thus an increasing of 19% between the two experimental stages.

Comparatively to these temperatures registered on structural elements, the plastic material components mounted on the 2nd link of the articulated arm are less influenced by the two experimental stages maintaining a

quite constant temperature between 29°C and 32°C depending of their location and the radiation level of the previously specified main heat sources (driving motors).

7. CONCLUSIONS

Present paper has presented experimental research performed for an ABB IRB 120 robot, targeting as main objectives the identification of most important heat sources and the thermal field distribution analysis as well as appropriate specific causes explaining robot thermal behavior. Main results obtained from experimental research and data processing confirm initially assumptions on heat sources identification and supply important information about thermal field distribution. Specific external maximum temperature of each IR's partially assembly and the thermal field distribution on each IR's partially assembly were clearly identified as well as their temperature variations along both specific programmed experimentally work cycles.

REFERENCES

- [1] *IRB 120-Rev.I-ROBO149EN_Data Sheet Rev. 1 January 2019*, available at: <https://new.abb.com/products/robotics/industrial-robots/irb-120>, accessed: 2019-09-15.
- [2] *Product specification IRB 120*, available at: <https://new.abb.com/products/robotics/industrial-robots/irb-120>, accessed: 2019-09-15.
- [3] *Product manual, spare parts - IRB 120*, available at: <https://new.abb.com/products/robotics/industrial-robots/irb-120>, accessed: 2019-09-15.
- [4] U. Heisel, F. Richter, K. H. Wurst, *Thermal Behavior of Industrial Robots and Possibilities for Error Compensation*, CIRP Annals, Vol. 46, Issue 1, 1997, pp. 283–286.
- [5] M. Cherif, J-Y. Knevez, A. Ballu, *Thermal Behavior of Industrial Robots and Possibilities for Error Compensation*, Proceedings of IDMME – Virtual concept 2010 Bordeaux, France October 2010, pp. 1–4.
- [6] Rui Li, Yang Zhao, *Dynamic error compensation for industrial robot based on thermal effect model*, Measurement, Vol. 88 (2016), pp. 113–120.
- [7] C. Mohnke, S. Reinkobera, E. Uhlmann, *Constructive methods to reduce thermal influences on the accuracy of industrial robots*, Procedia Manufacturing, Vol. 33 (2019) pp. 19–26.
- [8] C. Mohnke, S. Reinkobera, E. Uhlmann, *Articulated industrial robots: An approach to thermal compensation based on joint power*, International Conference and Exhibition on Laser Metrology, Machine Tool, CMM & Robotic Performance, Vol. 13 (2019), Sheffield, pp. 81–92.
- [9] A.F. Nicolescu, C. Cristoiu, C. Dumitraşcu, R. Parpala, *Recording procedure of thermal field distribution and temperature evolution on ABB IRB 140 industrial robot*, The 8th International Conference on Advanced Concepts in Mechanical Engineering, IOP Conf. Series: Materials Science and Engineering, Vol. 444 (2018), pp. 1–12, "Gheorghe Asachi" Technical University of Iasi, June 07–08, 2018.
- [10] * *FLIR ThermoCAM SC640 Technical specification*, available at: http://vision-mesures.fr/index.php?controller=attachment&id_attachment=50, accessed: 2006-10-25.